Biochemical and Biophysical Research Communications **290,** 749–755 (2002)
doi:10.1006/bbrc.2001.6243, available online at http://www.idealibrary.com on IDEAL®

Intact Vinculin Protein Is Required for Control of Cell Shape, Cell Mechanics, and *rac*-Dependent Lamellipodia Formation

Wolfgang H. Goldmann and Donald E. Ingber[1]
Department of Pathology and Department of Surgery, Children's Hospital, Harvard Medical School, Boston, Massachusetts 02115

Received December 6, 2001

Studies were carried out using vinculin-deficient F9 embryonic carcinoma (γ229) cells to analyze the relationship between structure and function within the focal adhesion protein vinculin, in the context of control of cell shape, cell mechanics, and movement. Atomic force microscopy studies revealed that transfection of the head (aa 1–821) or tail (aa 811–1066) domain of vinculin, alone or together, was unable to fully reverse the decrease in cell stiffness, spreading, and lamellipodia formation caused by vinculin deficiency. In contrast, replacement with intact vinculin completely restored normal cell mechanics and spreading regardless of whether its tyrosine phosphorylation site was deleted. Constitutively active *rac* also only induced extension of lamellipodia when microinjected into cells that expressed intact vinculin protein. These data indicate that vinculin's ability to physically couple integrins to the cytoskeleton, to mechanically stabilize cell shape, and to support *rac*-dependent lamellipodia formation all appear to depend on its intact three-dimensional structure.

Key Words: **motility; cytoskeleton; cytoskeletal mechanics; focal adhesion; G protein.**

Cell spreading and motility are made possible through binding of cell surface integrin receptors that transmit contractile forces from the cytoskeleton, across the cell surface, and to the extracellular matrix (ECM) adhesive substrate (1, 2). Integrins mechanically couple to the cytoskeleton through binding to cytoskeletal-associated proteins which assemble together to form focal adhesion complexes (3, 4). Focal adhesions also function as major sites for transduction of signals elicited by integrin binding, including those which control cell shape and movement (5, 6).

Past studies have revealed that the focal adhesion protein, vinculin, plays a central role in mechanical coupling of integrins to the cytoskeleton as well as in related control of cytoskeletal mechanics, cell shape, and motility (7–9). For example, deletion of vinculin from wild type (WT) F9 embryonic carcinoma cells using chemical mutagenesis resulted in production of vinculin-deficient cells that only spread to half the size of the WT cells; reintroduction of vinculin into these cells by transfection also reversed this effect (10). Another vinculin-deficient F9 cell line produced by homologous recombination to selectively target and disrupt the expression of both copies of the vinculin gene—γ229 cells—also spread less on fibronectin (FN) (9, 11). The decreased spreading of vinculin-deficient cells was accompanied by reduced stress fiber formation, formation of fewer focal adhesions, and inhibition of lamellipodia extension (8, 10). However, there was little or no reduction in the number of filopodia (7) which, like lamellipodia, form as a result of actin polymerization. In addition, mechanical analysis of γ229 cells using atomic force microscopy (AFM) and magnetic twisting cytometry revealed a progressive decrease in cytoskeletal stiffness (increase in flexibility) of the integrin-cytoskeleton linkage as the total amount of vinculin was decreased in F9 cells (12). Importantly, all of these behaviors (cell spreading, lamellipodia extension, formation of focal adhesions and stress fibers, and cytoskeletal stiffness) returned to normal when vinculin-deficient γ229 cells were transfected with vinculin (10, 12). Thus, vinculin's ability to mechanically couple integrins to the cytoskeleton within the focal adhesion appears to be critical for control of cytoskeletal mechanics, cell spreading, and lamellipodia formation in F9 cells.

[1] To whom correspondence and reprint requests should be addressed at Enders 1007—Children's Hospital, Department of Surgery and Department of Pathology, Harvard Medical School, 300 Longwood Avenue, Boston, MA 02115. Fax: 617 232-7914. E-mail: donald.ingber@tch.harvard.edu.

0006-291X/02 $35.00

While vinculin's role in forming a mechanical linkage between integrins and the actin cytoskeleton is well known, the molecular mechanism by which it can influence lamellipodia extension remains unknown. Given that lamellipodia formation appears to be driven by activation of the small G protein, *rac* (13, 14), past findings from studies with vinculin-deficient cells suggest that vinculin's structural coupling to integrins must in some way influence the signal transduction machinery that involves *rac*. This possibility is consistent with the observation that *rac*-induced lamellipodia are generated through localized actin polymerization at the cell periphery in regions that are enriched for vinculin-containing focal adhesions (15, 16) where migrating cells exert tractional forces on the substrate (17). Thus, in this study we explored whether vinculin is required for *rac* activation.

Vinculin is a large protein that contains multiple binding domains for other cytoskeletal proteins and focal adhesion components as well as phosphorylation sites that could contribute to its effects on lamellipodia formation and cell migration. The protein contains 1066 amino acids (aa) and consists of a head and a tail region which may physically interact to mask binding sites for other proteins (18–20). The head domain contains binding sites for α-actinin and talin as well as a tyrosine phosphorylation site while the tail domain contains binding sites for actin, paxillin, and lipids. F9 cell lines have been created which express either the head fragment of vinculin (aa 1–821), the tail (aa 811–1066), both fragments simultaneously, or the intact vinculin molecule (aa 1–1066) (9, 11). Expression of the head or tail domain of vinculin, either alone or in combination, is not sufficient to restore normal attachment or spreading in these cells. These studies raise the possibility that the vinculin molecule must be intact and that correct spatial relationships must be maintained between its different internal binding domains for normal cell shape control. In the present study, we explored this possibility by using atomic force microscopy (AFM) to quantitate the effects of different vinculin fragments on cell shape and cytoskeletal mechanics.

Vinculin also may become phosphorylated on tyrosine 822, however, its importance for control of cell shape and movement remains unclear. For example, although vinculin is known to be a target of *v-src*, it is not clear whether vinculin tyrosine phosphorylation plays a role in the changes in cell shape or adhesivity that are induced by this viral tyrosine kinase (21). A small amount of phosphorylated vinculin associates with the platelet cytoskeleton when the cells are activated by thrombin or by any stimulus that raises Ca^{2+} levels; this association correlates with secretion and clot retraction, but not with substrate adhesion (22). Similarly, while cell adhesion to ECM stimulates both focal adhesion kinase activity and binding of phosphorylated paxillin to tensin within focal adhesions, vinculin and talin do not become tyrosine-phosphorylated under these conditions (23). On the other hand, phosphotyrosinated vinculin appears to be necessary for cytoskeletal assembly during growth cone motility in cultured nerve cells (24). We therefore also examined the effects of transfecting a form of vinculin lacking the tyrosine phosphorylation site into vinculin-deficient γ229 cells and then compared their effects on cell behavior.

MATERIALS AND METHODS

Culture conditions. Wild-type mouse embryonic F9 carcinoma (WT) cells and a related cell line (γ229 cells) in which both vinculin genes were inactivated by homologous recombination (9) were generous gifts from Dr. E. D. Adamson (Burnham Institute, La Jolla, CA). Full-length mouse vinculin cDNA was generated by polymerase chain reaction (PCR) and stably transfected into γ229 cells using the calcium phosphate precipitation method to restore vinculin function (10). Fragments containing the sequences of the head and/or tail domain were subcloned into the same pCXN2 vector. Expression of the vinculin domain cDNAs was driven by a β-actin promotor plus 200 bp of an enhancer derived from CMV (11). The cells were maintained on 0.1% gelatin-coated culture dishes in high glucose (4 mg/L) DMEM, 10% calf serum, 20 mM Hepes, 2 mM L-glutamine, and 100 U/ml penicillin–streptomycin (12, 25). For experiments, cells were suspended with trypsin, washed in 1% BSA/DMEM and cultured in the same medium.

Atomic force microscopy. All F9 cell lines were cultured for 8 h on fibronectin-coated culture dishes (4 μg/35-mm dish). Prior to experimentation, the dishes were rinsed with PBS to remove non-adherent cells. Visualization of cell shape and quantitation of both projected cell areas and cell stiffness were accomplished using an atomic force microscope (AFM) from Digital Instruments (Santa Barbara, CA). This device has proven to be an effective tool for investigating the motility of living cells (26–28). A major advantage of this noninvasive method is its ability to detect dynamic changes in the viscoelastic properties of the cell with a high spatial resolution ($<$nm range). The AFM scans the cell surface using a sharp tip at the end of a cantilever. During force mapping, an image of the cells' surface topography is produced. The cantilever tip was positioned on the cell and its deflection was measured by a position-sensitive two-segment photodiode; the extent to which the applied force indents the cell depends on its elastic properties. The Hertz model was then used to describe the elastic response in relation to indentation and loading force (29). Between 4 and 5 cells were analyzed for each experimental condition. Cell stiffness profiles generated by force scans were transformed into 256 gray "stiffness" values (0–255). Stiffness profiles were generated by plotting pixel intensity (cell elasticity measured at each pixel) as a function of pixel distribution (frequency of pixels exhibiting each elasticity value). Two dimensional (2D) cell images were generated by translating the 256 gray stiffness values into 32 pseudocolors where 0 (red) and 255 (blue) corresponded to the least and most stiff values, respectively (as shown in the Stiffness Scale of Fig. 1).

Purification of Recombinant rac from Escherichia coli. cDNA encoding constitutively active human *rac* (1-V12) was generated by PCR and fused to the carboxy-terminal end of the GST gene by cloning into the *Bam*HI/*Eco*RI sites of pGEX-2T (30). The expression of fusion proteins was under the control of a tac promoter. After cleavage with thrombin, the GTPase has Gly-Ser-Pro fused to the second codon of the native sequence. The pGEX-2T vector containing *rac* was introduced into *E. coli* and stored as glycerol stock at -70°C. The stock solution was used to inoculate (1:100) *E. coli* containing

the expression plasmids and the cells were incubated overnight at 37°C. For microinjection, we dialyzed against 2 liters of 10 mM Tris–HCl, pH 7.6, 150 mM NaCl, 2 mM $MgCl_2$, and 0.1 mM DTT at 4°C overnight with one buffer change. Protein preparations (1 mg/ml) were stored in 10-μl aliquots in liquid nitrogen prior to use.

Microinjection. For microinjection studies, F9 cells were plated at a density between 1 and 2×10^5 cells per 35-mm well and cultured for 24 h in DMEM without serum prior to use. Cells were injected using an Eppendorf microinjector and micromanipulator. The flow in the microcapillary pipette was initiated with a brief pulse (<5 s) at high pressure (3000–4000 kPa) prior to microinjection (31, 32). Because of their small size and low amount of cytoplasm, these cells were then injected in manual mode; the pressure was set to 100–150 kPa to ensure a constant flow rate; approximately 1 ng of *rac* was injected per cell. Between 100 and 150 cells were injected within 10 min while being maintained on a heated microscope stage holder at 37°C. A thin film of mineral oil was spread on top of the medium to minimize gas exchange and maintain pH.

RESULTS

Vinculin-Dependent Control of Cell Shape and Mechanics

Past studies have shown that expression of partial fragments of vinculin within vinculin-deficient γ229 cells does not fully restore normal adhesion or spreading; only expression of intact vinculin protein is sufficient (11). To determine the relation between vinculin protein structure and function in the context of cytoskeletal mechanics and lamellipodia formation, we studied F9 cell lines that either contained wild-type vinculin (WT) or ones that completely lacked vinculin (γ229) which were then transfected with intact vinculin (F9 rescue), the head domain (aa 1–821; γ229 + head), the tail domain (aa 811–1066; γ229 + tail), or both the head and tail simultaneously (γ229 + head + tail). Levels of expression of the transfected vinculin proteins were between 83 and 100% of that exhibited by WT cells in all studies. AFM was then used to determine how the expression of these vinculin variants influenced F9 cell shape and mechanics.

AFM analysis confirmed that the vinculin-deficient γ229 cells spread less extensively (Figs. 1A and 1B) and exhibited approximately a 25% overall decrease in mechanical stiffness compared to WT cells (Table 1) whereas expression of intact vinculin protein reversed these effects (Fig. 1F, Table 1), as previously observed (12). Analysis of cells expressing individual vinculin fragments demonstrated that they also produced statistically significant increases in the mechanical resistance of γ229 cells as well as changes in cell shape (Figs. 1B–1E and Table 1). But analysis of the data revealed that reexpression of the head or tail domain alone produced only minimal (less than 8%; $P \leq 0.05$) increases in cell stiffness relative to that measured in γ229 cells. Simultaneous expression of both fragments resulted in an additive effect and increased stiffness by approximately 14% ($P \leq 0.02$), however, only expression of intact vinculin protein restored cell mechanics

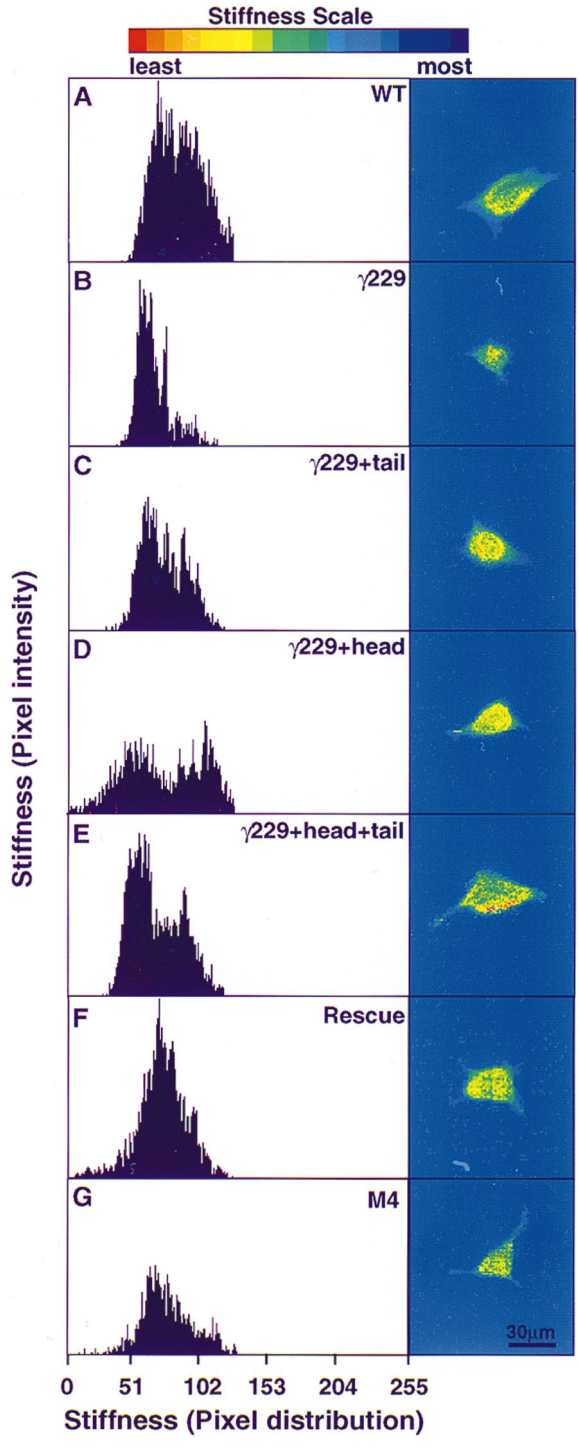

FIG. 1. AFM analysis of F9 cells expressing different forms of vinculin. Histograms of the pixel distributions representing the stiffness profiles (left) and corresponding 2D cell profile in pseudocolors generated by AFM force scans across the surface (right) of a representative WT (A), γ229 (B), γ229 + tail (C), γ229 + head (D), γ229 + head + tail (E), F9 rescue (F), and M4 (G) cell. Stiffness profiles were obtained as described under Materials and Methods; higher pixel distributions indicate greater mechanical stiffness. Color images of individual cells were generated by transferring the cell stiffness data into 32 pseudocolors, as indicated on the Stiffness Scale. Bar = 30 μm.

TABLE 1

Effects of Expression of Different Vinculin Forms on Cell Mechanics, as Determined by AFM

Cell type	Relative stiffness	±SD	Change (%)
γ229	64.46	3.22	
γ229 + head	68.26	2.60	5.9
γ229 + tail	69.49	1.72	7.8
γ229 + head + tail	73.09	1.62	13.4
M4	73.75	2.27	14.5
Rescue	79.47	2.07	23.4
WT	81.09	3.53	25.8

Note. Mean values for cell stiffness were calculated from the data obtained as shown in Fig. 1. Percentage increases in cell stiffness were based on the measured change in stiffness (pixel distribution; histogram) relative to that exhibited by vinculin-deficient γ229 cells. Mean values are presented ± SD; for all conditions, $P \leq 0.05$.

and spreading to levels similar to that observed in WT cells. M4 cells expressing a mutant vinculin in which the phosphorylation site (Tyr822) was changed to Phe also were able to spread and significantly increase their stiffness relative to γ229 cells (Fig. 1G and Table 1).

We and others (11, 12) have previously established that γ229 cells fail to spread because they are unable to produce stable lamellipodia and that this effect is due to the absence of vinculin. Because of the small size of γ229 cells, changes in lamellipodia extension may be measured by quantitating changes in total projected cell using AFM (33). Analysis of the AFM images of individual cells confirmed that the increases in cell spreading we observed were primarily due to extension of new lamellipodia (Figs. 1A–1H). When changes in cell area were quantitated in response to expressing the various forms of vinculin, we found that neither expression of the head nor the tail fragment was able to restore lamellipodia formation. Only when both the head and tail domains were expressed simultaneously in the same cell did we observe a significant increase in total area (approximately 65% compared to WT cells) (Fig. 2). In contrast, the F9 rescue and M4 cells (lacking the tyrosine phosphorylation site) which both expressed the entire vinculin molecule exhibited nearly identical projected cell areas to that displayed by WT cells. These data collectively demonstrate that structurally intact vinculin is necessary for maintenance of normal cell shape stability (mechanical stiffness) and effective formation of lamellipodia necessary for cell spreading whereas phosphorylation of Tyr822 is not required.

Vinculin-dependent control of rac action. Since the small G protein, rac, has been shown to drive lamellipodia extension (34, 35), we then asked whether the ability of different vinculin variants to modulate cell shape and mechanics correlates with their ability to support rac-dependent lamellipodia formation. Constitutively active rac 1-V12 was microinjected into serum-starved F9 cell lines. Within 10 s of injection, we detected membrane ruffling and within 20 min the average projected cell area increased by approximately 20% in WT cells due to extension of multiple lamellipodia (Figs. 3 and 4), a level of stimulation similar to that previously observed in 3T3 cells using a similar microinjection technique (32). In contrast, cell spreading increased by less than 8% in vinculin-deficient γ229 cells over the same time course (Fig. 4). We then determined the ability of constitutively active rac to induce lamellipodia protrusion by measuring changes in projected cell areas by phase contrast microscopy after its microinjection into γ229 cells expressing the different vinculin forms. The rac-induced increases in cell area were greatest in the WT and F9 rescue cells, lowest in the γ229 cells, slightly higher in γ229 + tail or γ229 + head cells, and intermediate in γ229 + tail/head cells (Fig. 4). These results, which were measured in response to microinjection of exogenous constitutively active rac, also correlated directly with the effects of expression of the various vinculin forms on spontaneous cell spreading and lamellipodia formation (Figs. 1A–1G). Finally, microinjection of rac into M4 cells produced lamellipodia formation at a level similar to that observed in WT cells, indicating that tyrosine phosphorylation of vinculin is not required for this response (Fig. 4). Taken together, these data indicate that only intact vinculin protein with its normal three dimensional conformation and structural coupling between its various binding sites can restore cell mechanics, cell shape control, and lamellipodia formation in vinculin-deficient F9 cells, and that tyrosine phosphorylation of vinculin is not required for these effects.

DISCUSSION

Cell adhesion to ECM and focal adhesion formation are important for control of cell shape, cytoskeletal mechanics, and motility. However, the molecular basis

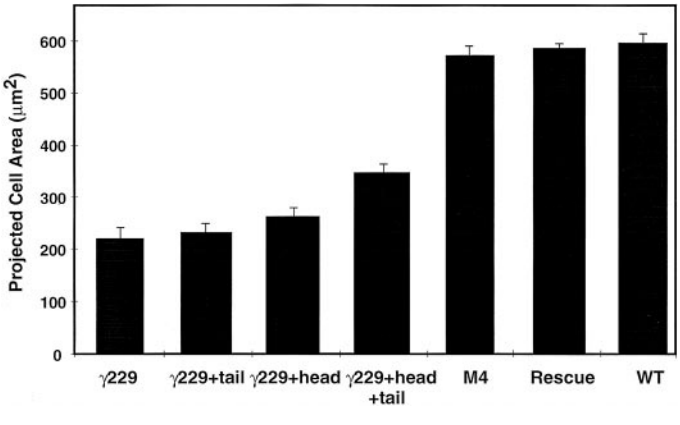

FIG. 2. Effects of expressing various vinculin forms on cell spreading (projected cell areas) as determined at 4 h after plating on fibronectin by AFM. Error bars indicate standard deviation (SD).

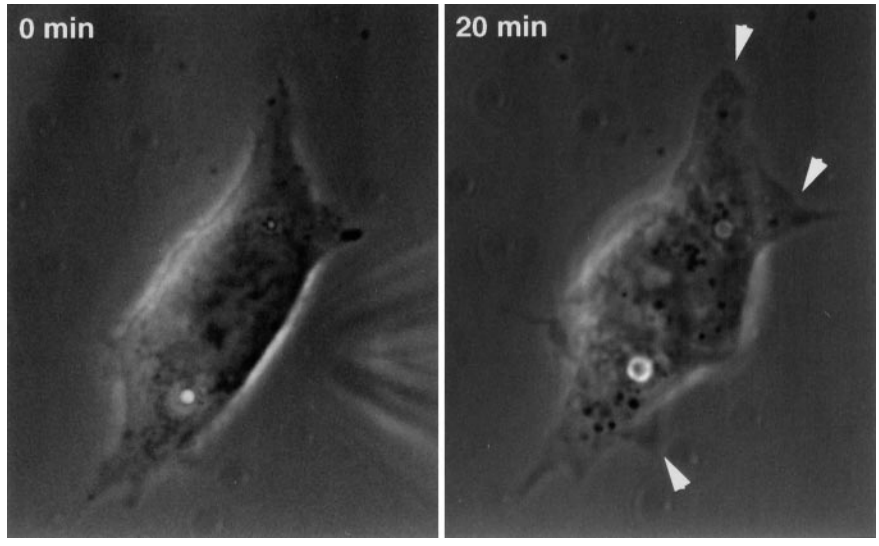

FIG. 3. Phase-contrast micrographs of WT cells at 0 (left) and 20 (right) min after microinjection of constitutively active *rac* 1-V12 (1 ng). Tips of arrowheads abut on an extending lamellipodium.

for this control remains poorly understood. Past work involving replacement of vinculin in vinculin-deficient cell lines by transfection has shown that the presence of this protein within focal adhesions is required to mechanically couple integrins to the cytoskeleton; this linkage is also necessary for cells to extend lamellipodia and spread (10, 12, 25). Previous studies involving transfection of head or tail domains of vinculin into vinculin-deficient γ229 cells revealed that only intact vinculin protein that retains normal head-tail interactions can fully restore cell adhesion and spreading (11). The results of the present study extend these findings by clarifying that phosphorylation of the tyrosine residue (aa 822) of vinculin is not required for these effects. However, the most novel finding of this study is that the intact vinculin protein is also required for normal signal transduction in F9 cells and, in particular, for activation of the *rac* signaling pathway which drives extension of lamellipodia.

Two conformations of vinculin have been described: an "open" configuration in which the globular head domain attaches to the tail such that it permits talin binding and a "folded" form in which the tail physically prevents access of talin to its binding site (18–20). The folded form also does not appear to bind actin, paxillin or α-actinin. The present results show that even though the head fragment of vinculin represents 77% of the whole molecule, contains both the talin and α-actinin binding sites, and lacks the inhibitory tail region, it contributed little to cell stiffness or lamellipodia formation when transfected into vinculin-deficient cells. The tail domain of vinculin that contains the paxillin and actin binding sites was equally ineffective. This is interesting given that these two unfolded vinculin fragments should be able to collectively bind talin, α-actinin, paxillin, and actin molecules that continue to localize within focal adhesions in vinculin-deficient γ229 cells (11).

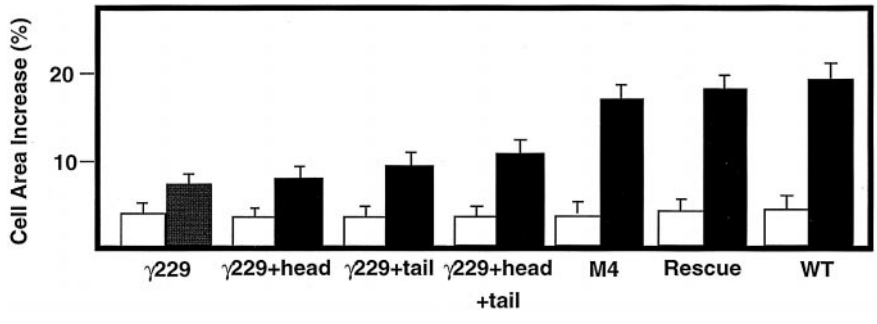

FIG. 4. Effects of expressing different vinculin forms on *rac*-dependent lamellipodia formation and cell spreading. γ229, γ229 + head, γ229 + tail, γ229 + head + tail, M4, F9 rescue, and WT cells were microinjected with PBS control (open bar) or constitutively active *rac* 1-V12 (solid bar) and projected cell areas were quantitated by computerized image analysis. Relative increases in cell spreading were calculated by comparing cell areas measured at 20 min to those obtained just prior to microinjection in the same cells.

While simultaneous administration of both fragments did significantly increase cell stiffness, spreading and lamellipodia formation, it could not fully restore normal behavior even though both molecules were expressed at nearly identical levels to intact vinculin in WT cells. These results suggest that vinculin must bind simultaneously to multiple focal adhesion molecules (e.g., talin and α-actinin as well as paxillin and actin) and possibly bring them together in space in order to mechanically couple integrins to the cytoskeleton and promote cell shape changes. Apparently, the efficiency of this process is greatly decreased when physical coupling between the head and tail regions of the vinculin molecule is lost. Only when full-length intact vinculin was expressed in F9 rescue cells were the true features of WT cells restored. Furthermore, removal of the tyrosine phosphorylation site of vinculin had no effect on cell spreading or lamellipodia formation and only a minimal effect on stiffness indicating that modification of this site by cellular tyrosine kinases is not required for these behaviors.

The finding that intact vinculin is required for lamellipodia formation suggests that efficient structural coupling between integrins and the cytoskeleton may be required for signal transduction events that normally drive this process. To explore this possibility, we microinjected the GTPase, *rac*, into F9 cells expressing the various vinculin forms. Again, these results correlated directly with those relating to vinculin's role in spontaneous cell spreading and control of cell mechanics. The head and tail fragments of vinculin had little effect on their own and an intermediate effect when combined; only when intact vinculin was re-introduced, was full responsiveness to *rac* restored. These results demonstrate that vinculin can modify the cell's signal transduction machinery and particularly, small G protein signaling, in addition to providing a structural anchoring role.

Although no direct regulatory function has been demonstrated for phosphorylated vinculin within living cells, past investigators have suggested that phosphorylation of tyrosine 822 of vinculin may play some role in *v-src* transformed cells (36). In spite of several attempts, it has not been possible to link the cytoskeletal changes that are observed following transformation to the tyrosine phosphorylation of vinculin, talin, paxillin, or β-integrin, all of which occur in these cells (3). The results of the present study confirm that phosphorylation of vinculin at tyrosine 822 is not required for maintenance of cell shape stability, cell spreading, or *rac*-induced lamellipodia formation, although it remains possible that phosphorylation of this site on vinculin could mediate activation of other signaling pathways.

We conclude that vinculin contributes to the mechanical integrity of the cytoskeleton and shape control by simultaneously binding multiple focal adhesion proteins and that the efficiency of this interaction is enhanced when the relevant binding sites of the head and tail are maintained in close proximity within the same molecule. Our data also reveal a previously unrecognized function of vinculin: the ability to locally modulate *rac* action and lamellipodia formation.

ACKNOWLEDGMENTS

We thank Nathan Busch for the use of the AFM, Markus Ludwig and Manfred Radmacher for helping with image analysis, and Sui Huang and Tom Polte for helpful editorial input. This work was supported by grants from NIH (CA-45548), NASA (NAG5-4839), and NATO (CRG 970205).

REFERENCES

1. Ingber, D. E. (1993) Cellular tensegrity: Defining new rules of biological design that govern the cytoskeleton. *J. Cell Sci.* **104,** 613–627.
2. Sheetz, M. P., Felsenfeld, D. P., and Galbraith, C. G. (1998) Cell migration: Regulation of force on extracellular-matrix–integrin complexes. *Trends Cell Biol.* **8,** 51–54.
3. Burridge, K., Fath, K., Kelly, T., Nuckolls, G., and Turner, C. (1988) Focal adhesions: Transmembrane junctions between the extracellular matrix and the cytoskeleton. *Annu. Rev. Cell Biol.* **4,** 487–525.
4. Wang, N., Butler, J. P., and Ingber, D. E. (1993) Mechanotransduction across the cell surface and through the cytoskeleton. *Science* **260,** 1124–1127.
5. Plopper, G. E., McNamee, H. P., Dike, L. E., Bojanowski, K., and Ingber, D. E. (1995) Convergence of integrin and growth factor receptor signaling pathways within the focal adhesion complex. *Mol. Biol. Cell* **6,** 1349–1365.
6. Miyamoto, S., Katz, B. Z., Lafrenie, R. M., and Yamada, K. M. (1998) Fibronectin and integrins in cell adhesion, signaling, and morphogenesis. *Ann. N.Y. Acad. Sci.* **857,** 119–129.
7. Samuels, M., Ezzell, R. M., Cardozo, T. J., Critchley, D. R., Coll, J. L., and Adamson, E. D. (1993) Expression of chicken vinculin complements the adhesion-defective phenotype of a mutant mouse F9 embryonal carcinoma cell. *J. Cell Biol.* **121,** 909–921.
8. Goldmann, W. H., Schindl, M., Cardozo, T. J., and Ezzell, R. M. (1995) Motility of vinculin-deficient F9 embryonic carcinoma cells analyzed by video, laser confocal, and reflection interference contrast microscopy. *Exp. Cell Res.* **22**1, 311–319.
9. Coll, J. L., Ezzell, R. M., Rodriguez Fernandez, J. L., Baribault, H., Oshima, R. G., and Adamson, E. D. (1995) Targeted disruption of vinculin genes in F9 and embryonic stem cells changes cell morphology, adhesion, and locomotion. *Proc. Natl. Acad. Sci. USA* **92,** 9161–9165.
10. Ezzell, R. M., Goldmann, W. H., Wang, N., Parasharama, N., and Ingber, D. E. (1997) Vinculin promotes cell spreading by mechanically coupling integrins to the cytoskeleton. *Exp. Cell Res.* **231,** 14–26.
11. Xu, W., Coll, J. L., and Adamson, E. D. (1998) Rescue of the mutant phenotype by reexpression of full-length vinculin in null F9 cells: Effects on cell locomotion by domain deleted vinculin. *J. Cell Sci.* **111,** 1535–1544.
12. Goldmann, W. H., Galneder, R., Ludwig, M., Xu, W., Adamson, E. D., Wang, N., and Ezzell, R. M. (1998) Differences in elasticity of vinculin-deficient F9 cells measured by magnetometry and atomic force microscopy. *Exp. Cell Res.* **239,** 235–242.
13. Ridley, A. J., and Hall, A. (1992) The small GTP-binding protein

rho regulates the assembly of focal adhesions and actin stress fibers in response to growth factors. *Cell* **70,** 389–399.

14. Ridley, A. J., Paterson, H. F., Johnston, C. L., Diekmann, D., and Hall, A. (1992) The small GTP-binding protein rac regulates growth factor-induced membrane ruffling. *Cell* **70,** 401–410.
15. Hotchin, N. A., and Hall, A. (1995) The assembly of integrin adhesion complexes requires both extracellular matrix and intracellular rho/rac GTPases. *J. Cell Biol.* **131,** 1857–1865.
16. Nobes, C. D., and Hall, A. (1995) Rho, rac, and cdc42 regulate the assembly of multi-molecular focal complexes associated with actin stress fibers, lamellipodia, and filopodia. *Cell* **81,** 53–62.
17. Pelham, R. J., and Wang, Y. L. (1999) High resolution detection of mechanical forces exerted by locomoting fibroblasts on the substrate. *Mol. Biol. Cell* **10,** 935–945.
18. Johnson, R. P., and Craig, S. W. (1994) An intramolecular association between the head and tail domains of vinculin modulates talin binding. *J. Biol. Chem.* **269,** 12611–12619.
19. Johnson, R. P., and Craig, S. W. (1995). F-actin binding site masked by the intramolecular association of vinculin head and tail domains. *Nature* **373,** 261–264.
20. Johnson, R. P., and Craig, S. W. (2000) Actin activates a cryptic dimerization potential of the vinculin tail domain. *J. Biol. Chem.* **275,** 95–105.
21. Sefton, B. M., Hunter, T., Ball, E. H., and Singer, S. J. (1981) Vinculin: A cytoskeletal target of the transforming protein of Rous sarcoma virus. *Cell* **24,** 165–174.
22. Horvath, A. R., Muszbek, L., and Kellie, S. (1992) Translocation of pp60c-src to the cytoskeleton during platelet aggregation. *EMBO J.* **11,** 855–861.
23. Bockholt, S. M., and Burridge, K. (1993) Cell spreading on extracellular matrix proteins induces tyrosine phosphorylation of tensin. *J. Biol. Chem.* **268,** 14565–14567.
24. Igarashi, M., and Komiya, Y. (1991) Subtypes of protein kinase C in isolated nerve growth cones: Only type II is associated with the membrane skeleton from growth cones. *Biochem. Biophys. Res. Commun.* **178,** 751–757.
25. Goldmann, W. H., Galneder, R., Ludwig, M., Kromm, A., and Ezzell, R. M. (1998b) Differences in F9 and 5.51 cell elasticity determined by cell poking and atomic force microscopy. *FEBS Lett.* **424,** 139–142.
26. Keller, D., Chang, L., Lou, K., Singh, S., and Yorganciogla, M. (1992) Scanning force microscopy of cells and membrane proteins. *Proc. SPIE* **1639,** 91–101.
27. Radmacher, M., Tilmann, R. W., Fritz, M., and Gaub, H. E. (1992) From molecules to cells—Imaging soft samples with the AFM. *Science* **257,** 1900–1905.
28. A-Hassan, E., Heinz, W. F., Antonik, M. D., D'Costa, N. P., Nageswaran, S., Schoenenberger, C. A., and Hoh, J. H. (1998) Relative microelastic mapping of living cells by atomic force microscopy. *Biophys. J.* **74,** 1564–1578.
29. Radmacher, M., Fritz, M., Kacher, C. M., Cleveland, P. K., and Hansma, P. K. (1996) Measuring the viscoelastic properties of human platelets with the atomic force microscope. *Biophys. J.* **70,** 556–567.
30. Self, A., and Hall, A. (1995) Purification of recombinant rho/rac/G25K from *E. coli. Methods Enzymol.* **256,** 3–10.
31. Ridley, A. J. (1995) Microinjection of Rho and Rac into quiescent Swiss 3T3 cells. *Methods Enzymol.* **256,** 313–320.
32. Ridley, A. J. (1998) Mammalian cell microinjection assay to study the function of Rac and Rho. *Methods Mol. Biol.* **84,** 153–160.
33. Xu, W., Baribault, H., and Adamson, E. D. (1998b) Vinculin knockout results in multiple organ defects during embryonic development. *Development* **125,** 327–337.
34. Ridley, A. J., and Hall, A. (1992) The small GTP-binding protein rho regulates the assembly of focal adhesions and actin stress fibers in response to growth factors. *Cell* **70,** 389–399.
35. Ridley, A. J., Paterson, H. F., Johnston, C. L., Diekmann, D., and Hall, A. (1992) The small GTP-binding protein rac regulates growth factor-induced membrane ruffling. *Cell* **70,** 401–410.
36. Hamaguchi, M., and Hanafusa, H. (1987) Association of p60src with Triton X-100-resistant cellular structure correlates with morphological transformation. *Proc. Natl. Acad. Sci. USA* **84,** 2312–2316.